PCCP

ROYAL SOCIETY OF CHEMISTRY

PAPER

View Article Online
View Journal | View Issue

Cite this: *Phys. Chem. Chem. Phys.*, 2022, **24**, 22453

A crossed molecular beams and computational study on the unusual reactivity of banana bonds of cyclopropane (c-C_3H_6; X^1A_1') through insertion by ground state carbon atoms ($C(^3P_j)$)†

Galiya R. Galimova,‡[a] Alexander M. Mebel, *[a] Shane J. Goettl, ‡[b] Zhenghai Yang[b] and Ralf I. Kaiser *[b]

The mechanism and chemical dynamics of the reaction of ground electronic state atomic carbon $C(^3P_j)$ with cyclopropane c-C_3H_6 $\left(X^1A_1'\right)$ have been explored by combining crossed molecular beams experiments with electronic structure calculations of the pertinent triplet C_4H_6 potential energy surface and statistical computations of product branching ratios under single-collision conditions. The experimental findings suggest that the reaction proceeds *via* indirect scattering dynamics through triplet C_4H_6 reaction intermediate(s) leading to C_4H_5 product(s) plus atomic hydrogen *via* a tight exit transition state, with the overall reaction exoergicity evaluated as 231 ± 52 kJ mol^{-1}. The calculations indicate that $C(^3P_j)$ can easily insert into one of the three equivalent C–C 'banana' bonds of cyclopropane overcoming a low barrier of only 2 kJ mol^{-1} following the formation of a van der Waals reactant complex stabilized by 15 kJ mol^{-1}. The carbon atom insertion into one of the six C–H bonds is also feasible *via* a slightly higher barrier of 5 kJ mol^{-1}. These results highlight an unusual reactivity of cyclopropane's banana C–C bonds, which behave more like unsaturated C–C bonds with a π-character than saturated σ C–C bonds, which are known to be generally unreactive toward the ground electronic state atomic carbon such as in ethane (C_2H_6). The statistical theory predicts the overall product branching ratios at the experimental collision energy as 50% for 1-butyn-4-yl, 33% for 1,3-butadien-2-yl, i-C_4H_5, and 11% for 1,3-butadien-1-yl, n-C_4H_5, with i-C_4H_5 (230 kJ mol^{-1} below the reactants) favored by the C–C insertion providing the best match with the experimentally observed reaction exoergicity. The $C(^3P_j)$ + c-C_3H_6 reaction is predicted to be a source of C_4H_5 radicals under the conditions where its low entrance barriers can be overcome, such as in planetary atmospheres or in circumstellar envelopes but not in cold molecular clouds. Both i- and n-C_4H_5 can further react with acetylene eventually producing the first aromatic ring and hence, the reaction of the atomic carbon with c-C_3H_6 can be considered as an initial step toward the formation of benzene.

Received 18th July 2022,
Accepted 6th September 2022

DOI: 10.1039/d2cp03293g

rsc.li/pccp

1. Introduction

Unsaturated and hydrogen-deficient resonance stabilized hydrocarbon free radicals (RSFRs) play an important role in the growth of polycyclic aromatic hydrocarbons (PAH), which in turn serve as precursors of soot and carbonaceous particles in various environments spanning from high-temperature combustion flames[1–9] and circumstellar envelopes to low-temperature planetary atmospheres and the interstellar medium (ISM).[10–18] The first stage of the PAH growth process is the formation of the first aromatic ring (benzene, C_6H_6; phenyl, C_6H_5) or two fused aromatic rings such as naphthalene ($C_{10}H_8$) from non-aromatic hydrocarbons, which is followed by their further enlargement through addition of extra six- or five-membered rings.[3,19] Both stages often proceed through the reactions involving RSFRs.[20–25] For example, the first aromatic ring is predominantly produced either *via* the odd C_n route, *i.e.*, through the recombination of two propargyl radicals, C_3H_3,[26–30] and the i-C_5H_3 + CH_3 reaction,[31] or *via* the even C_n route including the reactions like n-C_4H_3 + C_2H_2, n/i-C_4H_5 + C_2H_2,[3] and C_4H_6 + C_2H/C_2.[32,33] The contribution of each of those reactions to the first aromatic ring formation depends on the conditions and the abundances of the radicals involved. But what is the original

[a] *Department of Chemistry and Biochemistry, Florida International University, Miami, FL 33199, USA. E-mail: mebela@fiu.edu*
[b] *Department of Chemistry, University of Hawai'i at Mānoa, Honolulu, HI 96822, USA. E-mail: ralfk@hawaii.edu*

† Electronic supplementary information (ESI) available. See DOI: https://doi.org/10.1039/d2cp03293g

‡ Both authors contributed equally to this work.

source of RSFRs themselves? In high temperature environments, they are produced by thermal decomposition of closed-shell hydrocarbons and accumulate due to their significantly higher stability and lower reactivity as compared to conventional free radical species. Alternatively, in low temperature conditions of ISM and planetary atmospheres photolysis may substitute the pyrolysis and also, RSFRs can be synthesized *via* bimolecular reactions of carbon atoms and small carbon clusters with unsaturated hydrocarbons.[34,35] Among them, the bimolecular reactions of ground-state carbon atoms $C(^3P_j)$ with unsaturated hydrocarbons are of special importance because of the high abundance of atomic carbon in the Universe. Carbon atoms have been detected and identified in significant amounts *via* their 609 μm $^3P_1$–$^3P_0$ transition in circumstellar envelopes of the carbon stars IRC + 10 216 and α Orionis,[36–39] the proto planetary nebulae, such as CRL 618 and CRL 2688,[40] as well as in the diffuse cloud ζOph[41] and the dense cloud OMC-1.[42] Carbon atoms have been demonstrated both experimentally and theoretically to react with unsaturated hydrocarbons rapidly even at very low temperatures and to generate, through these reactions, a variety of RSFRs including C_3H_3,[30,43] C_4H_3,[9,44,45] and C_4H_5.[34,35,46] Theoretical calculations of the corresponding potential energy surfaces (PES) show that the reactions begin with the addition of $C(^3P_j)$ to the π electronic density of an unsaturated hydrocarbon without an entrance barrier and then proceed to highly exoergic products *via* intermediates and transition states residing lower in energy than the initial reactants. A representative example is the reaction of $C(^3P_j)$ with the propylene molecule CH_2CHCH_3 which was found, using crossed molecular beam and kinetic experiments and computational studies, to produce C_4H_5 isomers 1-methylpropargyl, 3-methylpropargyl, and i-C_4H_5 (1,3-butadien-2-yl), *via* C-for-H replacement channels, as well as propargyl + CH_3.[46–49]

In a sharp contrast to unsaturated hydrocarbons, atomic carbon in its ground electronic state is nearly unreactive with saturated hydrocarbons. Only superthermal $C(^3P_j)$ atoms generated by laser ablation of graphite and possessing an energy of 2 eV and higher could react with H_2, HCl, HBr, CH_3OH,[50,51] and CH_4[52] according to experiments. The rate constant for the reaction of thermal $C(^3P_j)$ with methane was evaluated to be less than 5×10^{-15} cm^3 $molecule^{-1}$ s^{-1} or even much lower at room temperature,[53–55] and no room or lower temperature reactivity is known for the ground state atomic carbon with ethane (C_2H_6) or propane (C_3H_8). This is due to the fact that the reaction barriers for insertion of $C(^3P_j)$ into a single bond and for a direct H abstraction from a saturated molecule are high; for example, in the $C(^3P_j) + CH_4$ reaction the computed barriers are 51 and 113 kJ mol^{-1} for the insertion and abstraction channels, respectively.[56] An isomer of the unsaturated hydrocarbon propylene, cyclopropane c-C_3H_6 $\left(X^1A_1'\right)$, is formally a saturated hydrocarbon but it is peculiar nevertheless.

Cyclopropane is a ring molecule with bent C–C single bonds known as 'banana' bonds. Cyclopropane cannot maintain conventional pure sigma bonds, since c-C_3H_6 is a small cyclic molecule with three carbon atoms forming an equilateral triangle. The banana bonds in cyclopropane create interorbital angles of 104°, although the expected value for the triangular molecular shape is 60°. The C–C bonds in cyclopropane are weakened due to the bent bonds phenomenon, despite the fact that they are shorter than an ordinary C–C bond in a conventional alkane (1.51 Å *versus* 1.53 Å). Moreover, owing to some electron donation from the CH_2 groups the C–C bonds in cyclopropane also acquire a partial π character. Therefore, the reactivity of c-C_3H_6 is anticipated to be different from that of normal alkanes. This is indeed exemplified by the reaction mechanism of cyclopropane with $O(^1D)$ which, according to crossed molecular beams experiments and PES calculations, can barrierlessly proceed by insertions of the atomic oxygen to both C–H and C–C bonds,[57,58] whereas the reactions of $O(^1D)$ with small normal alkanes such as ethane and propane are dominated by the insertions only into C–H bonds.[59,60] But how the banana bonds in c-C_3H_6 behave with respect to much less reactive ground electronic state atomic carbon remains unknown. Is $C(^3P_j)$ capable to readily attack the banana C–C bonds just like it does with double C=C and triple C≡C bonds in unsaturated hydrocarbons or is it as unreactive as with normal alkanes?

The goal of the present work is to answer the above questions and to also assess the ability of the $C(^3P_j)$ plus c-C_3H_6 $\left(X^1A_1'\right)$ reaction to produce resonance stabilized C_4H_5 radicals *via* a C-for-H replacement channel characteristic for the reactions of the ground-state atomic carbon with unsaturated hydrocarbons and thus to contribute to the PAH formation and growth by generating important RSFR precursors to the first aromatic ring. This goal is achieved by revealing the chemical dynamics of the elementary reaction of $C(^3P_j)$ with c-C_3H_6 $\left(X^1A_1'\right)$ under single collision conditions in crossed molecular beams. In combination with electronic structure and RRKM calculations, the results propose the prevalent formation of resonance stabilized isomers of the C_4H_5 radicals *via* relatively low entrance barriers of a few kJ mol^{-1} for unusual atomic carbon insertions into the C–C and C–H bonds making this reaction potentially important in planetary atmospheres and circumstellar envelopes of carbon stars, although not for cold molecular clouds.

2. Experimental

Reactions of atomic carbon (C, ^3P_j) with cyclopropane (c-C_3H_6, X^1A_1', ≥99%, Sigma-Aldrich) were conducted under single collision conditions utilizing a universal crossed molecular beams machine.[61–65] Briefly, a pulsed supersonic beam of ground state carbon atoms was produced through a homemade laser ablation source exploiting a stepper motor (SP18074-3606) to rotate and helically translate a graphite rod[66–68] onto which the fourth harmonic output of a Nd:YAG laser (Quanta-Ray Pro 270, Spectra-Physics) operating at 30 Hz and 12 mJ per pulse was tightly focused to a spot size of less than 1.5 mm^2. The ablated carbon atoms were seeded in helium (He, 99.9999%, Airgas) at a backing pressure of 4 atm released by a Proch–Trickl[69] valve operating at 60 Hz with an amplitude of −400 V

and opening times of 80 μs. After entrainment of the ablated species, the beam passed through a skimmer and was velocity-selected by a four-slot chopper wheel. This resulted in a pulse characterized by a velocity, v_p, of 2209 ± 84 m s^{-1} and speed ratio, S, of 3.1 ± 0.2. The electronic states of atomic carbon have been determined previously; at the current velocity, carbon is only formed in its ^3P_j ground state.[66,70] The carbon beam crossed perpendicularly with a pulsed supersonic beam of cyclopropane (v_p = 812 ± 11 m s^{-1}, S = 11.6 ± 0.4) operated at 60 Hz with an amplitude of −400 V and backing pressure of 550 torr; this resulted in a collision energy, E_c, of 25.8 ± 1.9 kJ mol^{-1} and center-of-mass angle, Θ_{CM}, of 52.9 ± 1.4°. In addition to carbon atoms, laser ablation of the carbon rod results in dicarbon and tricarbon molecules.[6,35,71,72] Collision energies above 50 kJ mol^{-1} are required to initiate reactions involving tricarbon molecules,[73] therefore tricarbon does not react with cyclopropane. The reaction of dicarbon with cyclopropane was explored at higher mass-to-charge (m/z) ratios of 63, 64, and 65; however, no signal was found, indicating that dicarbon does not interfere with the title reaction under our experimental conditions.

Reactively scattered products were monitored by a triply differentially pumped universal detection system which is rotatable within the plane of the reactant beams. Upon entering the detector, neutral products are ionized by electron impact ionization at 80 eV at 2 mA before separation by a quadrupole mass filter (QC 150, Extrel) and amplification through a Daly type detector.[74] Up to 8.7 × 10^5 time-of-flight (TOF) spectra were accumulated at angles between 18 ≤ Θ ≤ 66° with respect to the carbon beam. The TOFs were integrated and normalized to extract the laboratory angular distribution. To obtain information on the reaction dynamics, the laboratory data were fit using a forward convolution routine.[75,76] This process transforms the data from the laboratory frame to the center-of-mass reference frame yielding the product translational energy, $P(E_T)$, and angular, $T(\theta)$, flux distribution in the center-of-mass (CM) reference frame. The CM functions define the product flux contour map which reveals the differential reactive cross section, $I(u,\theta) \sim P(u) \times T(\theta)$, as intensity with respect to the angle θ and the CM velocity u.[7]

3. Computational methods

The geometries of all species including reactants, products, intermediates and transition states involved in the C(^3P_j) plus c-C_3H_6 (X^1A_1') reaction were optimized using the hybrid density functional B3LYP[77,78] and the 6-311G(d,p) basis set.[79] Vibrational frequencies and zero-point energy (ZPE) corrections were calculated at the same level of theory. All stationary points were characterized as local minima or transition states (TSs) on the PES using the computed frequencies. Optimized Cartesian coordinates and calculated vibrational frequencies for all structures involved in the reaction are given in ESI.† The relative energies were refined using the explicitly correlated coupled clusters method[80,81] within the CCSD(T)-F12/cc-pVQZ-f12//B3LYP/6-311G(d,p)+ZPE(B3LYP/6-311G(d,p)) scheme; the typical accuracy of this approach is within 4 kJ mol^{-1} or better.[82] The Gaussian 09[83] and MOLPRO 2021[84] program packages were used for the *ab initio* calculations. The Rice–Ramsperger–Kassel–Marcus (RRKM) theory[85] was employed to calculate energy-dependent rate constants of individual unimolecular reaction steps following the formation of initial complexes. The rate constants were then used to compute product branching ratios under single-collision conditions using our in-house UNIMOL code.[86]

4. Results

4.1. Laboratory frame

The reaction of carbon (C, ^3P_j) with cyclopropane (c-C_3H_6, X^1A_1') was probed for atomic and molecular hydrogen loss channels. TOF spectra were collected at Θ_{CM} for m/z = 52 ($C_4H_4^+$) and 53 ($C_4H_5^+$), which are superimposable after scaling (Fig. 1). This indicates that only a single reaction channel is open in this elementary reaction; further, both masses arise from the same channel with signal at m/z = 52 originating from dissociative electron impact ionization of the neutral product at 53 amu. Since the ion counts of the parent ion at m/z = 53 ($C_4H_5^+$) were collected at a level of 13 ± 5% compared to the fragment ion at m/z = 52 ($C_4H_4^+$), the TOF spectra and laboratory angular distribution were acquired at the m/z of the highest signal-to-noise ratio, *i.e.* at m/z = 52 ($C_4H_4^+$). The TOF spectra (Fig. 2B) are very broad, typically ranging about 400 μs. The laboratory angular distribution (Fig. 2A) taken over the range of 18 ≤ Θ ≤ 66° features a slight asymmetry about the center-of-mass angle of 52.9 ± 1.4°, with greatest intensity about 5° lower than Θ_{CM}. This finding suggests the reaction of carbon (C, ^3P_j) with cyclopropane (c-C_3H_6, X^1A_1') proceeds *via* indirect scattering dynamics through C_4H_6 reaction intermediate(s) leading to C_4H_5 product(s) plus atomic hydrogen.

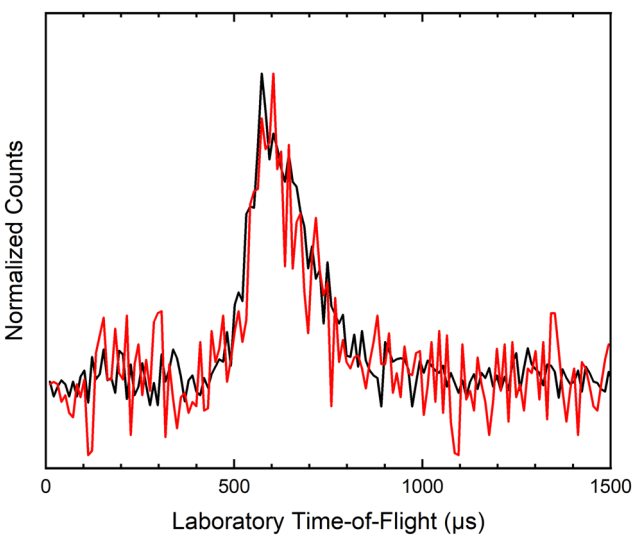

Fig. 1 Normalized time-of-flight (TOF) spectra recorded at m/z = 52 ($C_4H_4^+$, black) and 53 ($C_4H_5^+$, red) for the reaction of ground state atomic carbon (C, ^3P_j) with cyclopropane (c-C_3H_6, X^1A_1').

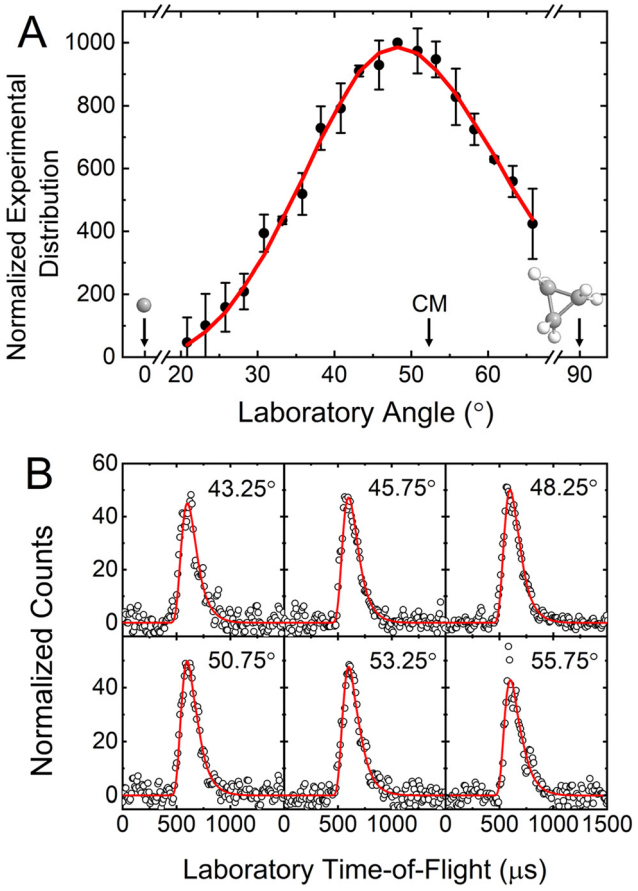

Fig. 2 Laboratory angular distribution (A) and time-of-flight (TOF) spectra (B) recorded at mass-to-charge (m/z) = 52 for the reaction of cyclopropane (c-C_3H_6) with ground state atomic carbon. CM represents the center-of-mass angle, and 0° and 90° define the directions of the carbon and cyclopropane beams, respectively. The black circles depict the data, red lines the fits, and error bars the 1σ standard deviation. Atoms are colored as follows: carbon (grey) and hydrogen (white).

4.2. Center-of-mass frame

To reveal the chemical dynamics of the carbon plus cyclopropane reaction, the experimental data were transformed from the laboratory reference frame to the CM reference frame. The TOF spectra and laboratory angular distribution were fit with a single channel corresponding to the formation of a molecule of the molecular mass 53 amu (C_4H_5) and atomic hydrogen; Fig. 3 shows the best-fit functions. The maximum product translational energy release, E_{max}, is obtained from the product translational energy distribution, $P(E_T)$ (Fig. 3A), with a derived value of 257 ± 50 kJ mol^{-1}. The conservation of energy dictates that the translational energy can be derived from the collision energy, reaction energy, and internal energy of the products, given by $E_T = E_c - \Delta_r G - E_I$. For those reaction products born without internal excitation (E_I), the reaction energy can be recovered with the formula $\Delta_r G = E_c - E_{max}$, which denotes a reaction exoergicity for the title reaction of 231 ± 52 kJ mol^{-1}. In addition, the $P(E_T)$ exhibits a maximum at 49 kJ mol^{-1}, indicating a tight exit transition state and a large rearrangement of electron density from the decomposing reaction intermediate to C_4H_5 and atomic hydrogen products.[87]

Additional information on the reaction dynamics can be obtained by inspecting the CM angular flux distribution, $T(\theta)$ (Fig. 3B). First, flux intensity is shown along the entire angular range, reinforcing the implication of indirect scattering dynamics through C_4H_6 intermediate(s). Second, the $T(\theta)$ features a slight forward scattering with an intensity ratio $I(0°)/I(180°)$ of about (1.5 ± 0.2) : 1.0, which suggests the existence of at least one channel where complex formation takes place but the lifetime is too short to allow multiple rotations.[88] These findings are also reflected in the flux contour map (Fig. 3C).

4.3. Potential energy surface

Our electronic structure calculations on the triplet C_4H_6 PES predict that atomic carbon can add barrierlessly to a carbon–carbon bond in cyclopropane forming a van der Waals complex lying 15 kJ mol^{-1} below the energy of the C(^3P_j) + c-C_3H_6 (X^1A_1') reactants (Fig. 4). Next, the reaction continues by insertion of the attacking C atom into the C–C bond leading to a four-membered ring intermediate **i1** (305 kJ mol^{-1} below the reactants) through a transition state (TS) residing 2 kJ mol^{-1} above the separated reactants. This result clearly indicates that the insertion of the ground state atomic carbon into a 'banana' C–C bond is a viable process. The **i1** intermediate can immediately lose a hydrogen atom from a CH_2 group adjacent to the attacking carbon radical leading to the four-membered ring C_4H_5 product **p5**, 139 kJ mol^{-1} lower in energy than the reactants through a TS lying 131 kJ mol^{-1} below the reactants. Also, the CH_2 group opposite to the bare C atom in **i1** can split an H atom, with simultaneous formation of a new C–C bond across the ring, thus producing **p7** which has a bicyclic (rhombic) geometry made of two fused three-membered rings. However, this process is expected to be less competitive than the formation of **p5** + H because the corresponding TS resides only 62 kJ mol^{-1} below the reactants and the exothermicity of the **p7** + H products is 68 kJ mol^{-1}. In alternative to the H losses, **i1** can also isomerize. One possible isomerization pathway is the formation of isomer **i2** (293 kJ mol^{-1} lower in energy than C + C_3H_6) *via* 1,2-H migration from CH_2 to the bare C atom through a TS lying 108 kJ mol^{-1} below the reactants. The newly formed **i2** intermediate can also form the **p5** + H products losing a hydrogen atom from any of the two CH groups *via* a TS located 123 kJ mol^{-1} below the reactants' level. The barrier to form another rhombic bicyclic C_4H_5 product **p6** by an H loss from **i2** is higher, with the corresponding TS at 85 kJ mol^{-1} relative to the reactants. In this case, a hydrogen atom is eliminated from one of the CH_2 groups and this is accompanied by the C–C bond formation between the carbon atom that lost H and the opposite carbon. However, if a new C–C bond does not form upon the H loss from CH_2 in **i2**, a more favorable four-membered ring product **p3**, –CH_2CHCHCH–, can be produced *via* a TS lying 155 kJ mol^{-1} below the reactants, with overall reaction exothermicity of 225 kJ mol^{-1}. The **i2** intermediate can also undergo a four-membered ring opening leading to the intermediate **i3** lying 410 kJ mol^{-1} lower in energy than C + C_3H_6 *via* a TS residing 203 kJ mol^{-1} below the reactants. Next, **i3** can rearrange into **i4**

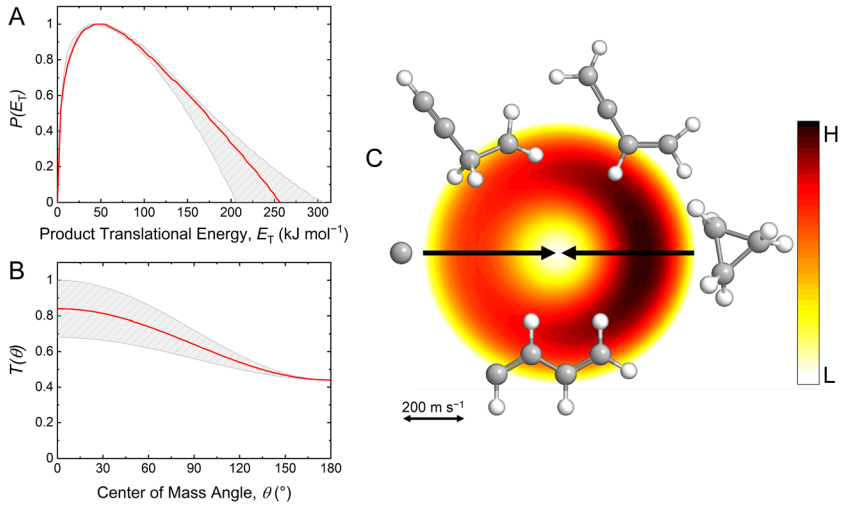

Fig. 3 CM translational energy (A) and angular (B) flux distributions, as well as the associated flux contour map (C) leading to the formation of C_4H_5 isomers plus atomic hydrogen in the reaction of ground state atomic carbon with cyclopropane (c-C_3H_6). Red lines define the best-fit functions while shaded areas provide the error limits. The flux contour map represents the intensity of the reactively scattered products as a function of product velocity (u) and scattering angle (θ), and the color bar indicates flux gradient from high (H) to low (L) intensity. Atoms are colored as follows: carbon (grey) and hydrogen (white).

(322 kJ mol^{-1} lower in energy than the reactants) by a hydrogen migration between two CH groups neighboring one another *via* a TS at 159 kJ mol^{-1} below the reactants. Alternatively, **i4** can form directly by the four-membered ring opening of **i1** *via* a TS located 183 kJ mol^{-1} lower in energy than C + C_3H_6. The intermediate **i4** can isomerize to its slightly more favorable conformer **i5** (323 kJ mol^{-1} below the reactants) by rotating the C=CH_2 group around a single C–C bond *via* a tiny barrier of 3 kJ mol^{-1}. The isomer **i5** can dissociate to the products **p2**, CH_2CHCCH_2 or i-C_4H_5 (230 kJ mol^{-1} below the energy of C_3H_6 + C), by losing one of the hydrogens from the central CH_2 group *via* a TS located 211 kJ mol^{-1} lower than the reactants and **p4**, CH_2CH_2CCH (175 kJ mol^{-1} below C + C_3H_6), by eliminating an H atom from the C=CH_2 group *via* a TS positioned 158 kJ mol^{-1} below the reactants. The central CH_2 group in **i5** can shift a hydrogen to the central H-less carbon atom leading to the intermediate **i6** (413 kJ mol^{-1} under the reactants' level), but the corresponding barrier (with TS lying 141 kJ mol^{-1} below the reactants) is significantly higher than those for the H losses from **i5**. Rotation around the central CH–CH bond in **i6** leads to its slightly more favorable conformer **i7** lying 414 kJ mol^{-1} below the reactants *via* a sizable barrier of 60 kJ mol^{-1}. **i7**, which appears to be the lowest energy minimum among all triplet C_4H_6 isomers considered here, can also be formed from the isomer **i3** by 90°-twisting of one of the symmetrically equivalent CH_2 groups around the corresponding CH–CH_2 bonds requiring a barrier of only 1 kJ mol^{-1}. This means that **i3** is likely to be only metastable with respect to its isomerization to **i7**. The isomer **i7** decomposes to the product **p2** by splitting a hydrogen atom from the CH group adjacent to the twisted CH_2 group, rotated 90° relative to the molecular plain, *via* a TS positioned 210 kJ mol^{-1} below the reactants. **i7** also can isomerize to the intermediate **i9** (393 kJ mol^{-1} below the reactants' level) through hydrogen migration from the CH group adjacent to the twisted CH_2 group to this CH_2 *via* a TS located 205 kJ mol^{-1} lower in energy than the reactants. The intermediate **i9** can also be obtained from **i4** *via* **i8** (386 kJ mol^{-1} lower in energy than the reactants) through a pathway involving an H shift from the central CH_2 group to the adjacent terminal CH_2 moiety overcoming a barrier at a TS lying 188 kJ mol^{-1} below the reactants, followed by another H migration from CH to bare C *via* a barrier at a TS located 186 kJ mol^{-1} lower in energy than the reactants. The intermediate **i9** dissociates to **p2** by eliminating a hydrogen atom from the CH_3 group *via* a TS lying 224 kJ mol^{-1} below the reactants. The intermediate **i8** can dissociate to the most exothermic propargyl C_3H_3 + CH_3 products (**p1**, 270 kJ mol^{-1} below the reactants) *via* the CH_3–CH bond cleavage (TS lying 228 kJ mol^{-1} lower in energy than the reactants). **i8** can also form **p2** through the hydrogen loss from the CH_3 group directly (TS at 210 kJ mol^{-1} under the level of C + C_3H_6) and through the two-step mechanism where the H loss is preceded by the *cis–trans* conformational change of **i8** to **i10** *via* a significant rotational barrier of 93 kJ mol^{-1}. The TS for the H loss from **i10** resides at 189 kJ mol^{-1} below the reactants.

The additional reaction channels leading to products **p8–p10** are illustrated in Fig. 5. The intermediate **i5** can form **i12** (309 kJ mol^{-1} below the energy of the reactants) by transferring a hydrogen atom from the CH_2 group to the neighboring central carbon *via* a TS located 117 kJ mol^{-1} below the reactants. **i12** can be also produced from **i1** *via* a metastable intermediate **i11** (100 kJ mol^{-1} lower in energy than the reactants) through the pathway involving the four-membered ring opening by a C–CH_2 bond cleavage (TS positioned 88 kJ mol^{-1} under the reactants' level) followed by the H migration from the central CH_2 group to the neighboring terminal bare carbon atom (TS lying 98 kJ mol^{-1}) below the reactants. The intermediate **i12** can undergo a change in conformation forming isomer **i14** (307 kJ mol^{-1} below the reactants) *via* rotation around the CH–CH bond (TS located 293 kJ mol^{-1} lower in energy than the reactants) and then **i14** can decompose to the **p10** products, triplet ethylene

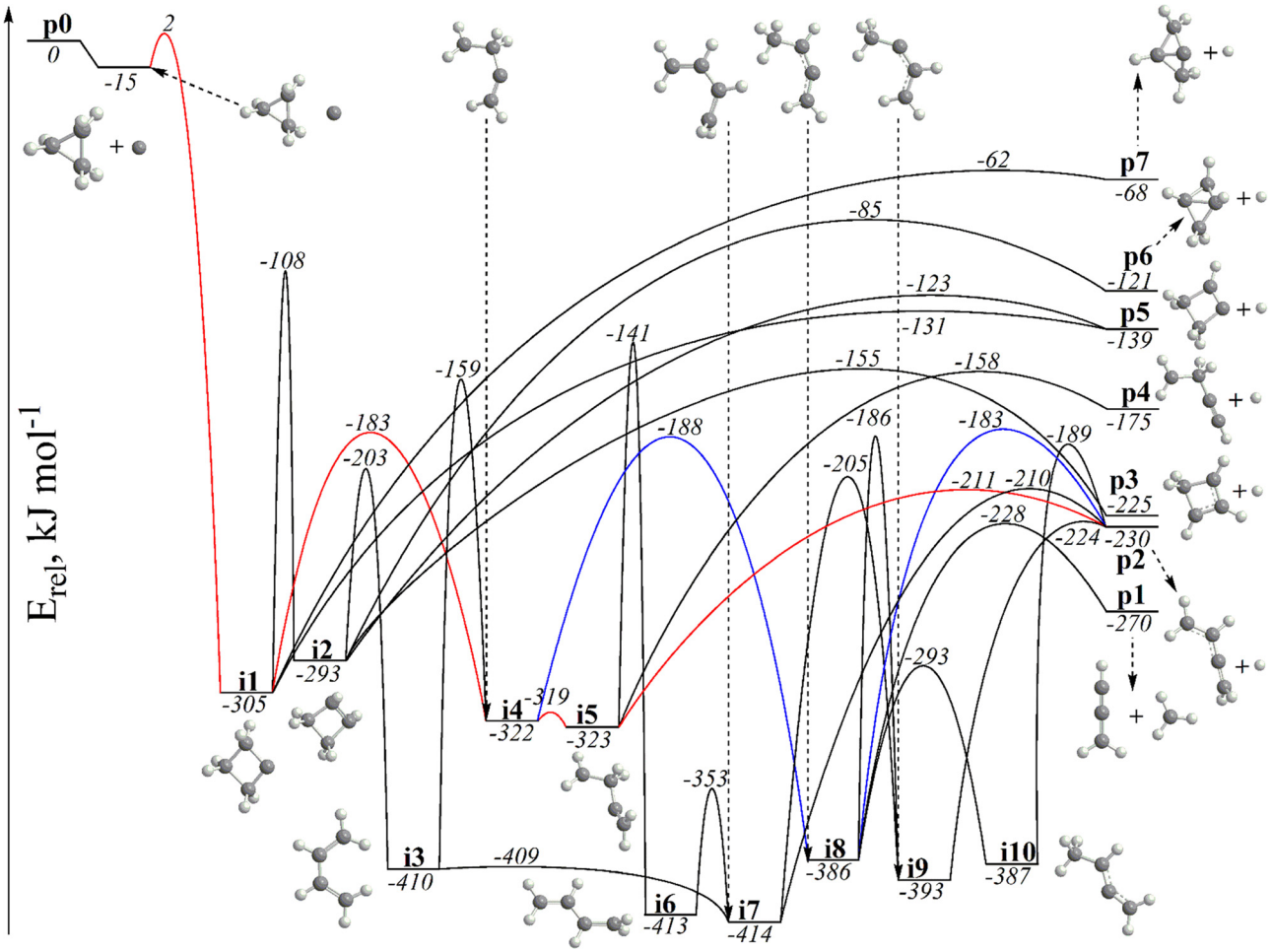

Fig. 4 Portion of the C_4H_6 PES leading to products **p1–p7** through intermediates **i1–i10**. The two preferable reaction pathways to **p2** are color coded in red and blue.

C_2H_4 plus acetylene C_2H_2, lying 211 kJ mol^{-1} below the reactants through the transition state lying 171 kJ mol^{-1} lower in energy than C + C_3H_6. The isomers **i8** and **i10** can dissociate to the 1-methylpropargyl product **p9** (229 kJ mol^{-1} below the reactants) by eliminating a hydrogen atom from the CH_2 group, with the corresponding TSs located 214 and 210 kJ mol^{-1} under the reactants' level, respectively. The isomer **i9** can undergo a conformational change to the intermediate **i13** (393 kJ mol^{-1} below C + C_3H_6) *via* overcoming a modest barrier of 26 kJ mol^{-1}. The 3-methylpropargyl product **p8** lying 240 kJ mol^{-1} below the energy of the reactants can be formed through a hydrogen elimination from the central carbon atoms in the intermediates **i13** and **i10** with the corresponding TSs residing 222 and 217 kJ mol^{-1} lower in energy than the reactants, respectively.

The atomic carbon can also insert into a C–H bond in cyclopropane forming **i15** lying 306 kJ mol^{-1} below the energy of the reactants (Fig. 6). In this case, the entrance barrier is calculated to be slightly higher than that for the insertion into the banana C–C bond, with the corresponding TS lying 5 kJ mol^{-1} above the reactants. The loss of a hydrogen atom from the CH group in the three-membered ring of **i15** leads to the formation of products **p13** + H (121 kJ mol^{-1} below the reactants). The same **p13** + H products can also be formed following isomerization of **i15** to **i16** (313 kJ mol^{-1} lower in energy than the reactants) by H migration from CH in the ring to the out-of-ring CH moiety overcoming a barrier with a TS 103 kJ mol^{-1} lower in energy than the reactants. The H loss TSs to produce **p13** + H from **i15** and **i16** respectively reside 109 and 112 kJ mol^{-1} under the reactants' level. The isomer **i16** can also split an H atom from a ring CH_2 group leading to the product **p12** lying 162 kJ mol^{-1} below the energy of the reactants *via* a TS located 103 kJ mol^{-1} below C + C_3H_6. The intermediate **i16** can ring-open to $CH_2CH_2CCH_2$, **i5** (323 kJ mol^{-1} below the reactants) *via* a TS positioned 264 kJ mol^{-1} lower in energy than the reactants, thus merging this section of the triplet C_4H_6 PES accessed *via* the C insertion into a C–H bond with the part of the surface accessed by C insertion into a C–C bond (Fig. 4 and 5). **i5** can rearrange to **i17**, CH_2CH_2CHCH, 307 kJ mol^{-1} below the reactants *via* hydrogen migration from the –C–CH_2 group to the central bare carbon atom through a TS located 124 kJ mol^{-1} below the reactants. The isomer **i17** can be formed more easily from the **i15** *via* ring opening with a TS lying 263 kJ mol^{-1} under C + C_3H_6. Then, **i17** can decompose to the products **p4** (175 kJ mol^{-1} lower in energy than the reactants) and **p11**,

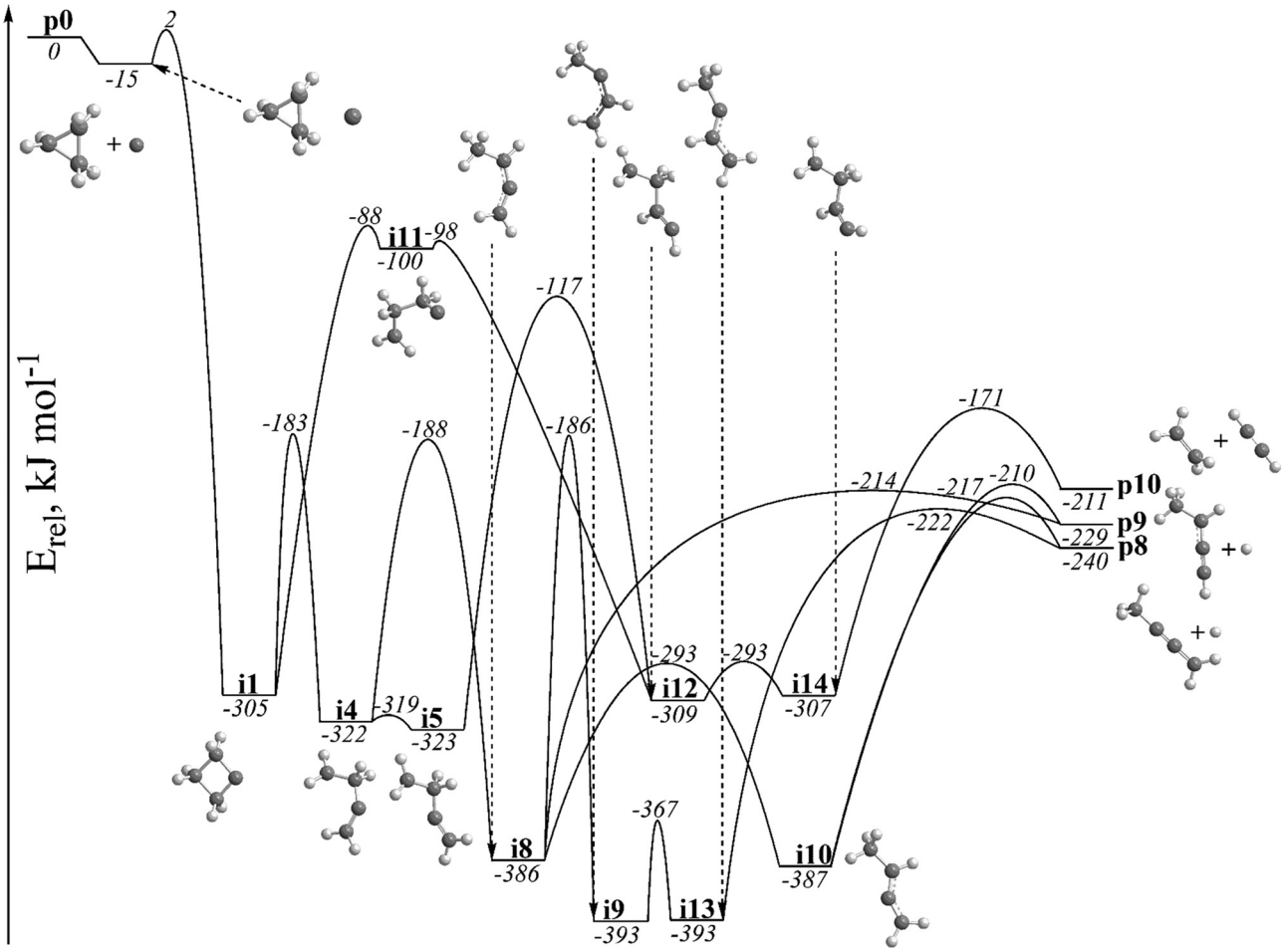

Fig. 5 Portion of the C_4H_6 PES leading to products **p8–p10** through intermediates **i1**, **i4–i5**, and **i8–i14**.

n-C_4H_5, 189 kcal mol^{-1} below the reactants, through hydrogen eliminations from the central CH and CH_2 groups *via* TSs residing 154 and 164 kJ mol^{-1} below the reactants' level, respectively. Clearly, the pathway C + C_3H_6 → **i15** → **i17** → **p4**/**p11** + H is the most favorable one following the C-atom insertion into a C–H bond.

5. Discussion and conclusions

We are now in position to combine the experimental and theoretical results and to unravel the mechanism of the C(^3P_j) plus c-C_3H_6 reaction. The experiment provides the reaction exoergicity of 231 ± 52 kJ mol^{-1} and points at an existence of a tight exit transition state connecting the decomposing triplet C_4H_6 intermediate to C_4H_5 plus H products. Several reaction products fall into this exoergicity range including **p2** (i-C_4H_5), **p3** (cyclobuten-3-yl), **p8** (3-methylpropargyl), **p9** (1-methylpropargyl), and **p11** (n-C_4H_5). All of these products are produced *via* tight transition states corresponding to distinct exit barriers in the range of 15–70 kJ mol^{-1}. The other, less exoergic C_4H_5 isomers can also be in principle produced as their signal can be buried under the slow portion of the experimental translational energy distribution. Looking at the PES accessed following the insertion of the attacking carbon atom into a C–C bond, one can see that the most energetically favorable reaction pathway leads to the formation of **p2**: C(^3P_j) + C_3H_6 → reactant complex → **i1** → **i4** → **i5** → **p2** + H. The critical TS for this channel beginning from **i1** is the one for the four-membered ring opening in this intermediate leading to **i4** located 183 kJ mol^{-1} under the reactants' level. The cyclobuten-3-yl product **p3** can be accessed by the H loss from **i2**, but the isomerization of **i1** is not competitive due the high barrier for **i1** → **i2**. The methylpropargyl products can form *via* the following pathways: C(^3P_j) + C_3H_6 → reactant complex → **i1** → **i4** → **i8** → (**i10** →) **p9** + H and C(^3P_j) + C_3H_6 → reactant complex → **i1** → **i4** → **i8** → **i10** → **p8** + H, but these channels are anticipated to be less competitive as compared to the production of **p2**, since the isomerization of **i4** to **i5** exhibits a much lower barrier than that to **i8**. The n-C_4H_5 product **p11** is likely to be formed *via* a pathway initiated by C-insertion into a C–H bond in cyclopropane: C(^3P_j) + C_3H_6 → **i15** → **i17** → **p11** + H. Interestingly, the **p4** product CH_2CH_2CCH (1-butyn-4-yl) whose exoergicity is just outside of the experimentally determined range could be competitive since it can form both from **i5** and **i17**, which are expected to be the main decomposing intermediates in the C–C and C–H insertion channels, respectively.

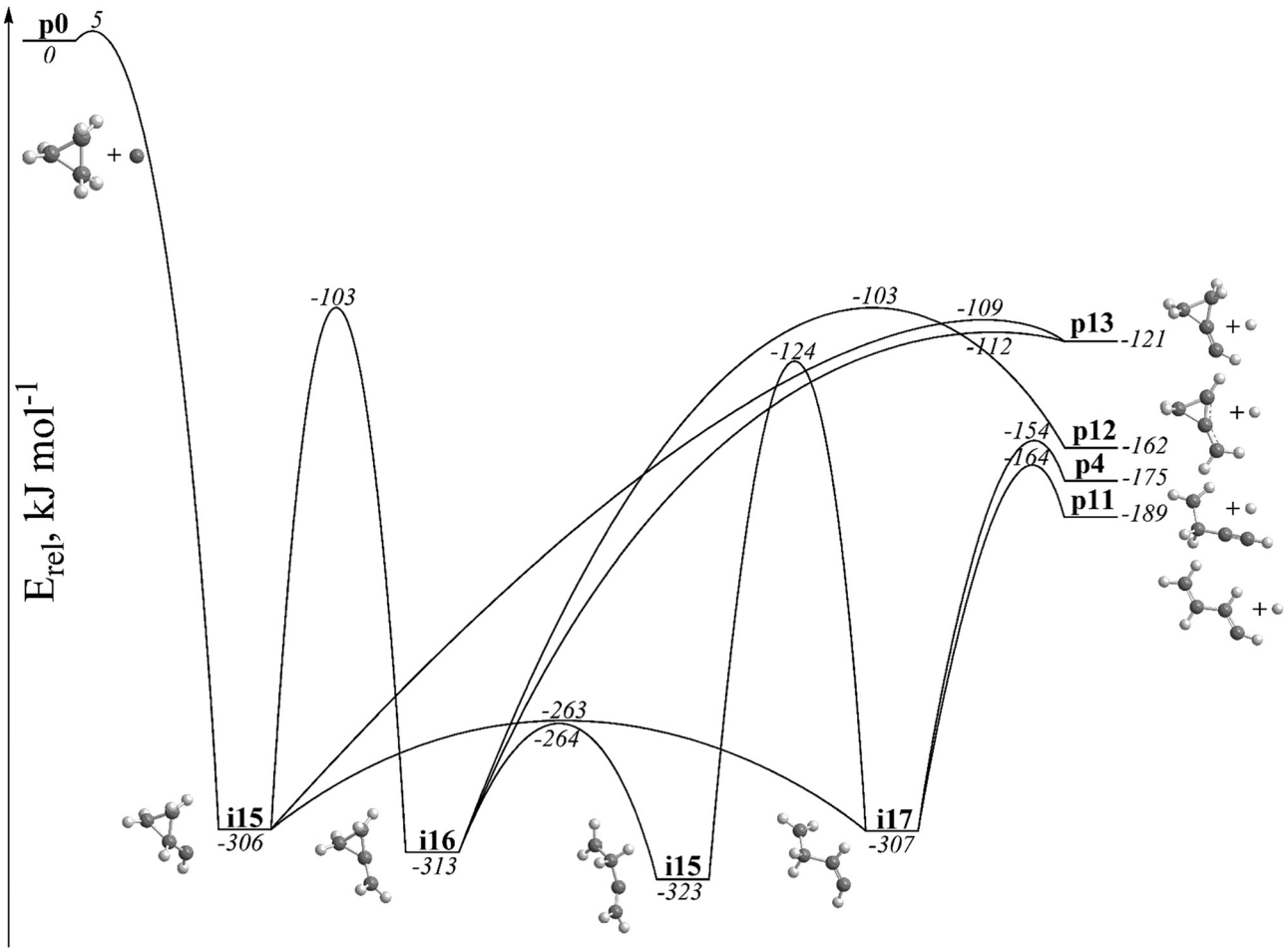

Fig. 6 Portion of the C_4H_6 PES leading to products **p4** and **p11–p13** through intermediates **i5** and **i15–i17**.

Statistical RRKM calculations of the product branching ratios corroborate the qualitative picture described above (Table 1). If the unimolecular reaction of the triplet C_4H_6 PES begins from intermediate **i1** following the C–C bond insertion, at the experimental collision energy, **p2** is predicted to be the main product (61%) followed by **p4** (27%), **p5** (7%), and propargyl + CH_3 (**p1**, 3%). The minor products are formed either from the same decomposing complex **i5** (**p4**), or from the initial complex **i1** (**p5**), or *via* the intermediates **i4** and **i8** (**p1**). Considering **i15** as the initial complex following the C-insertion into a C–H bond, **p4** and **p11** are predicted to be the main statistical products with the relative yields of 73% and 22%, respectively, with **p2** being a minor product at 4%. Here, both **p4** and **p11** are produced from the same decomposing complex **i17**, whereas **p2** is accessed from **i5**. Interestingly, the formation of **p4** from **i17** is favored by a looser TS despite the fact the H loss barrier toward **p11** is slightly lower than that leading to **p4**. From the energetic and molecular parameters of the entrance TSs for C-insertion into the C–C and C–H bonds, using RRKM rate constants to form **i1** and **i15** computed with an assumption that both pathways proceed from a common initial van der Waals complex, we can also evaluate the branching ratio in the entrance channel as 51%/49% where the slight energetic preference of the C–C insertion is nearly compensated by a factor of 2 higher reaction path degeneracy for the C–H insertion. Using the entrance channel branching ratio, the

Table 1 Statistical branching ratios (%) for the C + cyclopropane reaction at collision energies of 25.8 kJ mol^{-1}

	i1	**i15**	
Initial intermediate	100%	100%	Total[a]
p1	3.00	0.19	1.63
p2	61.06	4.00	33.28
p3	0.06	0.00	0.03
p4	27.32	73.26	49.69
p5	7.07	0.00	3.63
p6	0.00	0.00	0.00
p7	0.05	0.00	0.03
p8	0.18	0.01	0.10
p9	0.67	0.04	0.36
p10	0.29	0.00	0.15
p11	0.27	22.46	11.08
p12	0.02	0.00	0.01
p13	0.01	0.04	0.02

[a] Calculated using the 51.3%/48.7% branching in the entrance channel between the insertion of $C(^3P_j)$ into the C–C and C–H bonds, respectively.

statistical theory finally predicts the overall relative yields to be: **p4** (1-butyn-4-yl) – 50%, **p2** (1,3-butadien-2-yl, i-C_4H_5) – 33%, and **p11** (1,3-butadien-1-yl, n-C_4H_5) – 11%, with minor contributions from **p5** (cyclobuten-1-yl), and **p1** (propargyl + CH_3). Noteworthy is that the **p2** product matches the experimental reaction exoergicity best. This conclusion is also supported by a detailed inspection of two tight transition states leading to the **p2** product from intermediates **i5** and **i8** (Fig. 7). The forward scattered center of mass angular distribution requires that the incorporated carbon atom and leaving hydrogen atom must be located on opposite sides of the rotational axis.[89] This requirement is fully supported in both transition states connecting to **p2** (Fig. 7).

In our analysis so far, we considered only the triplet C_4H_6 PES initially accessed by the $C(^3P_j)$ reaction with c-C_3H_6 $\left(X^1A_1'\right)$. In the meantime, some intermediates on the most favorable reaction pathways, such as **i1**, **i4**, **i5**, **i8**, **i15**, and **i17** exhibit either carbene or biradical characters and therefore may have a close in energy singlet carbene or open-shell singlet states, respectively. In this case, intersystem crossing (ISC) from triplet to singlet PES could be in principle plausible. However, the present experimental results do not support any significant role of the singlet C_4H_6 surface in the reaction. First, the C_4H_5 products are formed *via* tight transition states with distinct exit barriers, whereas the decomposition of singlet C_4H_6 species to C_4H_5 + H should proceed without any exit barriers. Second, the most likely singlet intermediate to be produced after ISC is 1,3-butadiene, which could be formed, for example, from a singlet counterpart of **i1** *via* 1,2-H shift to the carbene site followed by facile ring opening in cyclobutene or by 1,2-H migration from CH_2 to the neighboring radical site in open-shell singlet **i4**/**i5**. The 1,3-butadiene molecule in this case would have internal energy of 657 kJ mol^{-1} [90] plus the collision energy which is comparable with 620 kJ mol^{-1} acquired by hot 1,3-butadiene in its photodissociation process at 193 nm after internal conversion to the ground electronic state. Our previous statistical calculations of product branching ratios of photodissociation of 1,3-butadiene at this wavelength showed a significant yield of H_2 loss C_4H_4 products along with C_4H_5, with the predicted H/H_2 loss branching ratio of 3.9/1.[91] In earlier crossed molecular beam experiments on the $C(^3P_j)$ + C_2H_2 reaction where ISC was found to play a role, H_2 elimination products were unambiguously detected.[92–97] Here, however, no such products were observed which corroborates a minor (if any) contribution of the singlet PES.

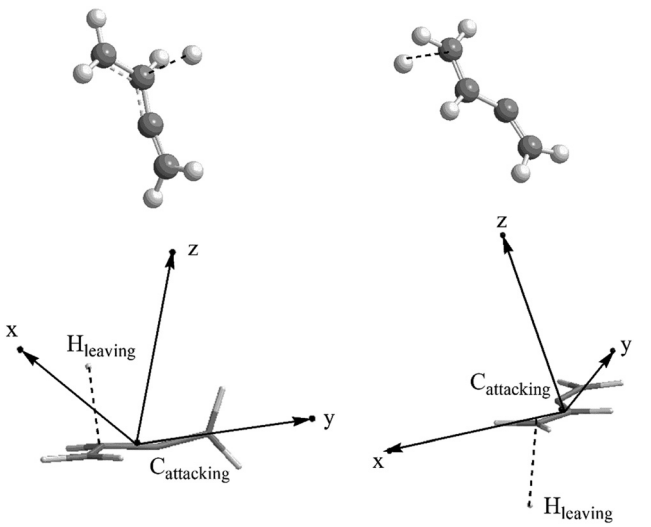

Fig. 7 Geometry of the transition states and the three principle rotational axes connecting intermediates **i5** (left) and **i8** (right) to **p2** in the preferable reaction pathways shown in Fig. 4.

Summarizing, the combined crossed molecular beams and computational study of the $C(^3P_j)$ reaction with cyclopropane shows the formation of C_4H_5 radicals together with atomic hydrogen *via* indirect scattering dynamics through triplet C_4H_6 intermediates. The prevailing reaction products include the resonance stabilized i-C_4H_5 radical as well as its n-C_4H_5 and 1-butyn-4-yl isomers. The banana bond in cyclopropane reacts with the ground state atomic carbon more like an unsaturated C–C bond with a π-character than a saturated σ C–C bond. While the saturated C–C bonds are generally unreactive toward $C(^3P_j)$, here we observe facile insertions of the atomic carbon both into the C–C and C–H bonds which require overcoming rather low barriers of few kJ mol^{-1}. Therefore, the $C(^3P_j)$ plus c-C_3H_6 reaction can serve as a source of C_4H_5 radicals under the conditions where those low barriers can be overcome, such as in planetary atmospheres or in circumstellar envelopes. Since both i- and n-C_4H_5 can in principle react with acetylene eventually producing the first aromatic ring, the reaction of the atomic carbon with c-C_3H_6 can be considered as an initial step toward the formation of C_6H_6. However, on the contrary to the reactions of $C(^3P_j)$ with unsaturated hydrocarbons, which proceed by barrierless additions of atomic carbon to π bonds, $C(^3P_j)$ + c-C_3H_6 exhibits small barriers both for the C–C and C–H insertion channels making this reaction too slow in the low-temperature conditions, such as in cold molecular clouds.

Conflicts of interest

There are no conflicts of interest to declare.

Acknowledgements

This work was supported by the U.S. Department of Energy, Basic Energy Sciences, by Grants No. DE-FG02-04ER15570 to the Florida International University and No. DE-FG02-03ER15411 to the University of Hawaii at Manoa.

References

1 H. Richter and J. B. Howard, *Prog. Energy Combust. Sci.*, 2000, **26**, 565–608.
2 M. J. Castaldi, N. M. Marinov, C. F. Melius, J. Hwang, S. M. Senkan, W. J. Pitz and C. K. Westbrook, *Symp. (Int.) Combust. Proc.*, 1996, **26**, 693–702.

3 M. Frenklach, *Phys. Chem. Chem. Phys.*, 2002, **4**, 2028–2037.
4 S. J. Goettl, C. He, D. Paul, A. A. Nikolayev, V. N. Azyazov, A. M. Mebel and R. I. Kaiser, *J. Phys. Chem. A*, 2022, **126**, 1889–1898.
5 A. M. Thomas, M. Lucas, T. Yang, R. I. Kaiser, L. Fuentes, D. Belisario-Lara and A. M. Mebel, *ChemPhysChem*, 2017, **18**, 1971–1976.
6 D. S. N. Parker, S. Maity, B. B. Dangi, R. I. Kaiser, A. Landera and A. M. Mebel, *Phys. Chem. Chem. Phys.*, 2014, **16**, 12150–12163.
7 R. I. Kaiser, *Chem. Rev.*, 2002, **102**, 1309–1358.
8 R. I. Kaiser, Y. T. Lee and A. G. Suits, *J. Chem. Phys.*, 1995, **103**, 10395–10398.
9 R. I. Kaiser, D. Stranges, Y. T. Lee and A. G. Suits, *Astrophys. J.*, 1997, **477**, 982–989.
10 Y. C. Minh and E. F. Dishoeck, *Astrochemistry – From Molecular Clouds to Planetary Systems*, ASP Publisher, San Francisco, 2000.
11 D. A. Williams, *Faraday Discuss.*, 1998, **109**, 1–14.
12 H. J. Fraser, M. R. S. McCoustra and D. A. Williams, *Astron. Geophys.*, 2002, **43**, 10–18.
13 R. I. Kaiser, C. Ochsenfeld, D. Stranges, M. Head-Gordon and Y. T. Lee, *Faraday Discuss.*, 1998, **109**, 183–204.
14 C. C. Chiong, O. Asvany, N. Balucani, Y. T. Lee and R. I. Kaiser, Proceedings of the 8th Asia-Pacific Physics Conference, 2001, pp. 167–169.
15 M. Frenklach, D. W. Clary, W. C. Gardiner and S. E. Stein, *Symp. (Int.) Combust., [Proc.]*, 1984, **20**, 887–901.
16 C. He, K. Fujioka, A. A. Nikolayev, L. Zhao, S. Doddipatla, V. N. Azyazov, A. M. Mebel, R. Sun and R. I. Kaiser, *Phys. Chem. Chem. Phys.*, 2022, **24**, 578–593.
17 R. I. Kaiser, X. Gu, F. Zhang and P. Maksyutenko, *Phys. Chem. Chem. Phys.*, 2012, **14**, 575–588.
18 D. S. N. Parker, T. Yang, R. I. Kaiser, A. Landera and A. M. Mebel, *Chem. Phys. Lett.*, 2014, **595**, 230.
19 M. Frenklach, D. W. Clary, W. C. Gardiner, Jr. and S. E. Stein, *Proc. Combust. Inst.*, 1988, **21**, 1067–1076.
20 J. A. Miller, *Symp. (Int.) Combust., [Proc.]*, 1996, **26**, 461–480.
21 N. M. Marinov, W. J. Pitz, C. K. Westbrook, M. J. Castaldi and S. M. Senkan, *Combust. Sci. Technol.*, 1996, **116/117**, 211–287.
22 J. A. Miller and C. F. Melius, *Combust. Flame*, 1992, **91**, 21–39.
23 A. D'Anna, A. Violi and A. D'Allesio, *Combust. Flame*, 2000, **121**, 418–429.
24 A. D'Anna and A. Violi, *Symp. (Int.) Combust., [Proc.]*, 1998, **27**, 425–433.
25 P. Lindstedt, *Symp. (Int.) Combust., [Proc.]*, 1998, **27**, 269–285.
26 J. A. Miller, *Faraday Discuss.*, 2001, **119**, 461–475.
27 J. A. Miller and S. J. Klippenstein, *J. Phys. Chem. A*, 2001, **105**, 7254–7266.
28 J. A. Miller and S. J. Klippenstein, *J. Phys. Chem. A*, 2003, **107**, 7783–7799.
29 L. Zhao, W. Lu, M. Ahmed, M. V. Zagidullin, V. N. Azyazov, A. N. Morozov, A. M. Mebel and R. I. Kaiser, *Sci. Adv.*, 2021, **7**, eabf0360.
30 R. I. Kaiser, Y. T. Lee and A. G. Suits, *J. Chem. Phys.*, 1996, **105**, 8705–8720.
31 A. M. Mebel, S. H. Lin, X. M. Yang and Y. T. Lee, *J. Phys. Chem. A*, 1997, **101**, 6781–6789.
32 B. M. Jones, F. Zhang, R. I. Kaiser, A. Jamal, A. M. Mebel, M. A. Cordiner and S. B. Charnley, *Proc. Natl. Acad. Sci. U. S. A.*, 2011, **108**, 452–457.
33 F. Zhang, B. Jones, P. Maksyutenko, R. I. Kaiser, C. Chin, V. V. Kislov and A. M. Mebel, *J. Am. Chem. Soc.*, 2010, **132**, 2672–2683.
34 R. I. Kaiser and A. M. Mebel, *Int. Rev. Phys. Chem.*, 2002, **21**, 307–356.
35 A. M. Mebel and R. I. Kaiser, *Int. Rev. Phys. Chem.*, 2015, **34**, 461–514.
36 J. Keene, K. Young, T. G. Phillips and T. H. Buttgenbach, *Astrophys. J.*, 1993, **415**, L131–L134.
37 W. E. C. J. Van Der Keen, P. J. Huggins and H. E. Matthews, *Astrophys. J.*, 1998, **505**, 749–755.
38 J. G. Ingalls, R. A. Chamberlin, T. M. Bania, J. M. Jackson, A. P. Lane and A. A. Stark, *Astrophys. J.*, 1997, **479**, 296–302.
39 C. D. Wilson, *Astrophys. J.*, 1997, **487**, L49–L52.
40 K. Young, *Astrophys. J.*, 1997, **488**, L157–L160.
41 U. J. Sofia, J. A. Cardelli, K. P. Guerin and D. M. Meyer, *Astrophys. J.*, 1997, **482**, L105–L108.
42 G. J. White and G. Sandell, *Astron. Astrophys.*, 1995, **299**, 179–192.
43 R. I. Kaiser, N. Balucani, D. O. Charkin and A. M. Mebel, *Chem. Phys. Lett.*, 2003, **382**, 112–119.
44 N. Balucani, A. M. Mebel, Y. T. Lee and R. I. Kaiser, *J. Phys. Chem. A*, 2001, **105**, 9813–9818.
45 R. I. Kaiser, D. Stranges, Y. T. Lee and A. G. Suits, *J. Chem. Phys.*, 1996, **105**, 8721–8733.
46 R. I. Kaiser, D. Stranges, H. M. Bevsek, Y. T. Lee and A. G. Suits, *J. Chem. Phys.*, 1997, **106**, 4945–4953.
47 R. I. Kaiser, T. L. Nguyen, T. N. Le and A. M. Mebel, *Astrophys. J.*, 2001, **561**, 858–863.
48 S. H. Lee, W. K. Chen, C. H. Chin and W. J. Huang, *J. Chem. Phys.*, 2013, **139**, 174–317.
49 J. C. Loison and A. Bergeat, *Phys. Chem. Chem. Phys.*, 2004, **6**, 5396–5401.
50 P. S. Skell, J. J. Havel and M. J. McGlinchey, *Acc. Chem. Res.*, 1973, **6**, 97–105.
51 M. R. Scholefield, S. Goyal, J. H. Choi and H. J. Reisler, *J. Phys. Chem.*, 1995, **99**, 14605–14613.
52 M. R. Scholefield, J. H. Choi, S. Goyal and H. J. Reisler, *Chem. Phys. Lett.*, 1998, **288**, 487–493.
53 F. F. Martinotti, M. J. Welch and A. P. Wolf, *Chem. Commun.*, 1968, 115–116.
54 W. Braun, A. M. Bass, D. D. Davis and J. D. Simmons, *Proc. R. Soc. London, Ser. A*, 1969, **312**, 417–434.
55 D. Husain and L. J. Kirsch, *Trans. Faraday Soc.*, 1971, **67**, 2025–2035.
56 G.-S. Kim, T. L. Nguyen, A. M. Mebel, S. H. Lin and M. T. Nguyen, *J. Phys. Chem. A*, 2003, **107**, 1788–1796.
57 J. Shu, J. J. Lin, C. C. Wang, Y. T. Lee, X. Yang, T. L. Nguyen and A. M. Mebel, *J. Chem. Phys.*, 2001, **115**, 7–10.

58 C. C. Wang, J. Shu, J. J. Lin, Y. T. Lee, X. Yang, T. L. Nguyen and A. M. Mebel, *J. Chem. Phys.*, 2002, **116**, 8292–8299.
59 J. Shu, J. J. Lin, Y. T. Lee and X. Yang, *J. Chem. Phys.*, 2001, **114**, 4–7.
60 J. Shu, J. J. Lin, Y. T. Lee and X. Yang, *J. Am. Chem. Soc.*, 2001, **123**, 322–330.
61 X. Gu, Y. Guo, F. Zhang and R. I. Kaiser, *J. Phys. Chem. A*, 2007, **111**, 2980–2992.
62 Y. Guo, X. Gu, F. Zhang, M. S. Tang, B. J. Sun, A. H. H. Chang and R. I. Kaiser, *Phys. Chem. Chem. Phys.*, 2006, **8**, 5454–5461.
63 Y. Guo, X. Gu, F. Zhang, B. J. Sun, M. F. Tsai, A. H. H. Chang and R. I. Kaiser, *J. Phys. Chem. A*, 2007, **111**, 3241–3247.
64 M. Lucas, A. M. Thomas, R. I. Kaiser, E. K. Bashkirov, V. N. Azyazov and A. M. Mebel, *J. Phys. Chem. A*, 2018, **122**, 3128–3139.
65 R. I. Kaiser, C. C. Chiong, O. Asvany, Y. T. Lee, F. Stahl, P. V. R. Schleyer and H. F. Schaefer III, *J. Chem. Phys.*, 2001, **114**, 3488.
66 R. I. Kaiser and A. G. Suits, *Rev. Sci. Instrum.*, 1995, **66**, 5405–5411.
67 X. Gu, Y. Guo, E. Kawamura and R. I. Kaiser, *J. Vac. Sci. Technol., A*, 2006, **24**, 505–511.
68 Y. Guo, X. Gu, E. Kawamura and R. I. Kaiser, *Rev. Sci. Instrum.*, 2006, **77**, 034701.
69 D. Proch and T. Trickl, *Rev. Sci. Instrum.*, 1989, **60**, 713–716.
70 R. I. Kaiser, A. M. Mebel and Y. T. Lee, *J. Chem. Phys.*, 2001, **114**, 231–239.
71 B. B. Dangi, D. S. N. Parker, R. I. Kaiser, D. Belisario-Lara and A. M. Mebel, *Chem. Phys. Lett.*, 2014, **607**, 92–99.
72 X. Gu, Y. Guo, A. M. Mebel and R. I. Kaiser, *Chem. Phys. Lett.*, 2007, **449**, 44–52.
73 Y. Guo, X. Gu, F. Zhang, A. M. Mebel and R. I. Kaiser, *Phys. Chem. Chem. Phys.*, 2007, **9**, 1972–1979.
74 N. R. Daly, *Rev. Sci. Instrum.*, 1960, **31**, 264–267.
75 M. F. Vernon, *Molecular Beam Scattering*, PhD thesis, University of California at Berkeley, Berkeley, CA, 1983.
76 P. S. Weiss, *Reaction Dynamics of Electronically Excited Alkali Atoms with Simple Molecules*, PhD thesis, University of California at Berkeley, Berkeley, CA, 1986.
77 A. D. Becke, *J. Chem. Phys.*, 1992, **97**, 9173–9177.
78 C. Lee, W. Yang and R. G. Parr, *Phys. Rev. B: Condens. Matter Mater. Phys.*, 1988, **37**, 785–789.
79 R. Krishnan, M. Frisch and J. A. Pople, *J. Chem. Phys.*, 1988, **72**, 4244–4245.
80 T. B. Adler, G. Knizia and H.-J. Werner, *J. Chem. Phys.*, 2007, **127**, 221106.
81 G. Knizia, T. B. Adler and H.-J. Werner, *J. Chem. Phys.*, 2009, **130**, 054104.
82 J. Zhang and E. F. Valeev, *J. Chem. Theory Comput.*, 2012, **8**, 3175–3186.
83 M. J. Frisch, G. W. Trucks, H. B. Schlegel, G. E. Scuseria, M. A. Robb, J. R. Cheeseman, G. Scalmani, V. Barone, B. Mennucci and G. A. Petersson, *Gaussian 09 Revision A.1*, Gaussian, Inc., Wallingford CT, USA, 2009.
84 H. J. Werner, P. J. Knowles, R. Lindh, F. R. Manby, M. Schütz, P. Celani, T. Korona, G. Rauhut, R. D. Amos and A. Bernhardsson, *MOLPRO, version 2021.1, A Package of Ab Initio Programs*, University of Cardiff, Cardiff, UK, 2021, see **https://www.molpro.net**.
85 H. Eyring, S. H. Lin and S. M. Lin, *Basis Chemical Kinetics*, John Wiley & Sons, Ltd., New York, NY, 1980.
86 C. He, L. Zhao, A. M. Thomas, A. N. Morozov, A. M. Mebel and R. I. Kaiser, *J. Phys. Chem. A*, 2019, **123**, 5446–5462.
87 S. A. Safron, N. D. Weinstein, D. R. Herschbach and J. C. Tully, *Chem. Phys. Lett.*, 1972, **12**, 564–568.
88 W. B. Miller, S. A. Safron and D. R. Herschbach, *Discuss. Faraday Soc.*, 1967, **44**, 108–122.
89 R. I. Kaiser, C. Ochsenfeld, M. Head-Gordon, Y. T. Lee and A. G. Suits, *Science*, 1996, **274**, 1508–1511.
90 B. Ruscic, *Active Thermochemical Tables, Version 1.122*, available at **https://atct.anl.gov**.
91 H. Y. Lee, V. V. Kislov, S. H. Lin, A. M. Mebel and D. M. Neumark, *Chem. – Eur. J.*, 2003, **9**, 726–740.
92 R. I. Kaiser, T. N. Le, T. L. Nguyen, A. M. Mebel, N. Balucani, Y. T. Lee, F. Stahl, P. V. R. Schleyer and H. F. Schaefer III, *Faraday Discuss.*, 2001, **119**, 51–66.
93 L. Cartechini, A. Bergeat, G. Capozza, P. Casavecchia, G. G. Volpi, W. D. Geppert, C. Naulin and M. Costes, *J. Chem. Phys.*, 2002, **116**, 5603–5611.
94 X. Gu, Y. Guo, F. Zhang and R. I. Kaiser, *J. Phys. Chem. A*, 2007, **111**, 2980–2992.
95 N. Balucani, J. Capozo, F. Leonori, E. Segoloni and P. Casavecchia, *Int. Rev. Phys. Chem.*, 2006, **25**, 109–163.
96 M. Costes, N. Daugey, C. Naulin, A. Bergeat, F. Leonori, E. Segoloni, R. Petrucci, N. Balucani and P. Casavecchia, *Faraday Discuss.*, 2006, **133**, 157–176.
97 A. Bergeat and J.-C. Loison, *Phys. Chem. Chem. Phys.*, 2001, **3**, 2038–2042.